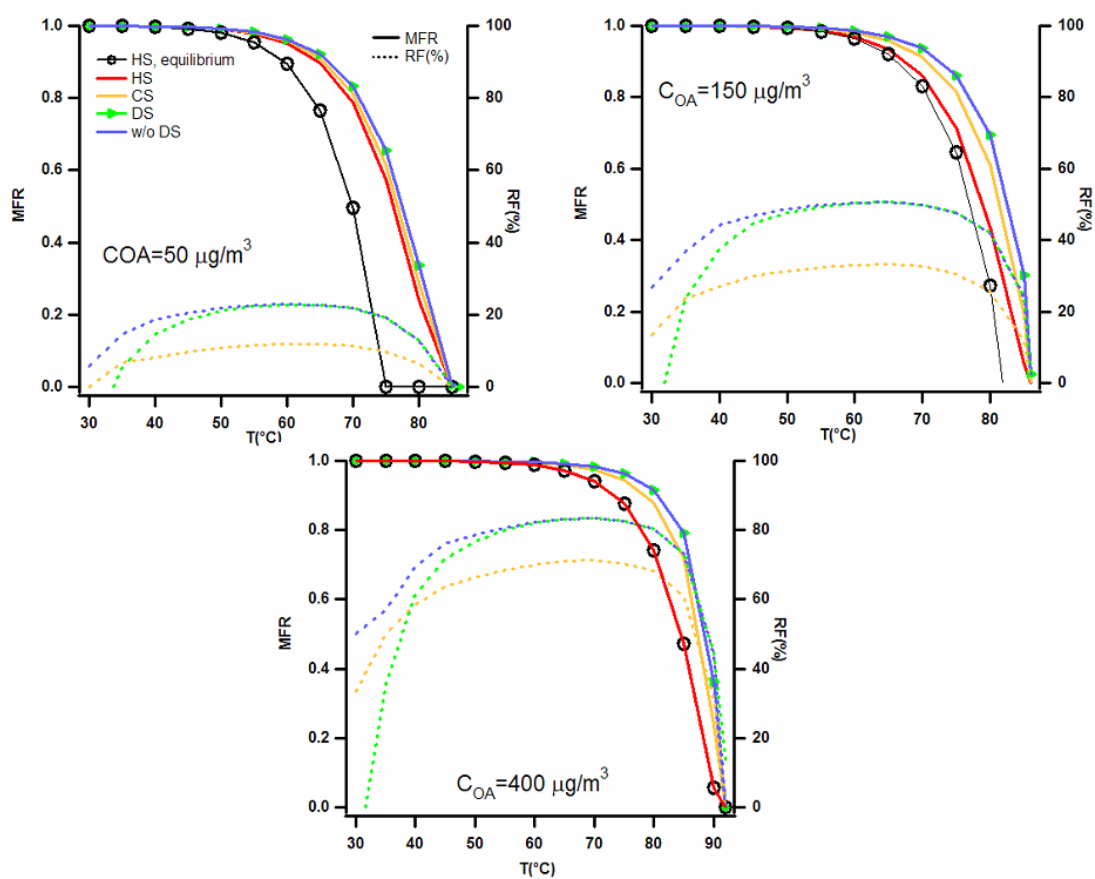
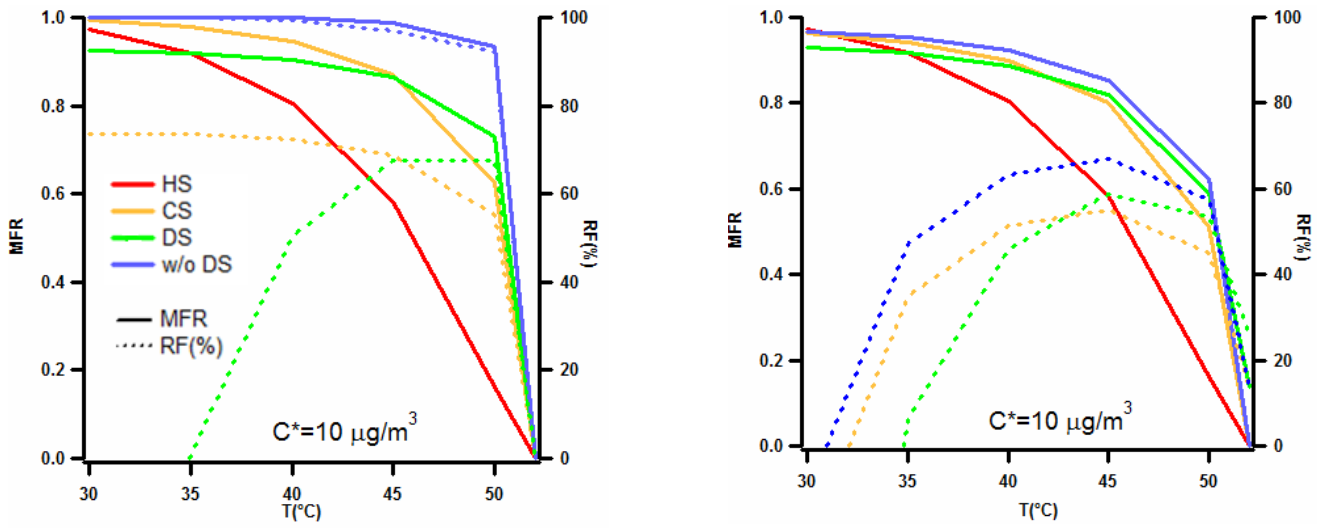


**Figure S1.** Example of spatial temperature distribution for the thermodenuder model configuration in this study. Initial temperature=25° C, wall temperature= 100°C.



**Figure S2.** Lower estimates of re-condensation as a function of aerosol mass loading. Plots represent output thermograms (MFR) and re-condensation fraction (RF) for the heating section (HS), cooling section (CS), denuder section (DS) and equivalent configuration without denuder section (w/o DS). Baseline case:  $C_{sat} = 0.01 \mu\text{g}/\text{m}^3$ ,  $dp = 100 \text{ nm}$ ,  $Di = 5 \times 10^{-6} \text{ m}^2/\text{s}$  and  $\gamma' = 1$ .



**Figure S3:** Upper (left) and lower (right) estimates of re-condensation for the case with  $C_{\text{sat}}=10 \mu\text{g}/\text{m}^3$ ,  $C_{\text{OA}}=400 \mu\text{g}/\text{m}^3$ ,  $d_p=100 \text{ nm}$ ,  $D_i=5 \times 10^{-6} \text{ m}^2/\text{s}$  and  $\gamma'=1$ . Plots represent thermograms and re-condensation fraction for the heating section (HS), cooling section (CS), denuder section (DS) and equivalent configuration without denuder section (w/o DS).

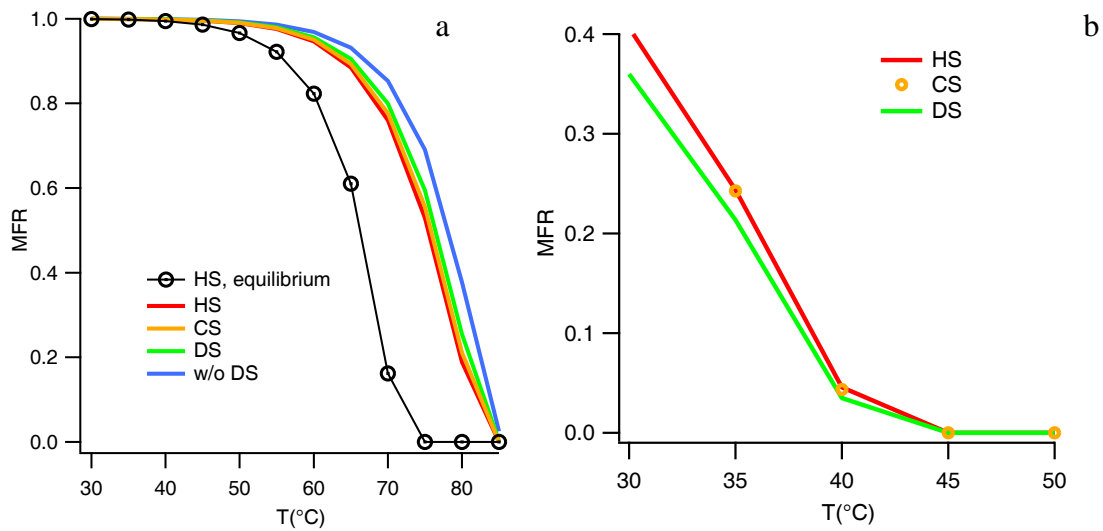


**Figure S4.** (a) Heating section (HS), cooling section (CS), denuder section (DS) and cooling section without denuder (w/o DS) output thermograms for  $30 \mu\text{g}/\text{m}^3$  aerosol mass loading. Baseline case:  $C^*=0.01 \mu\text{g}/\text{m}^3$ ,  $d_{p0}=100 \text{ nm}$ ,  $D_i=5 \times 10^{-6} \text{ cm}^2/\text{s}$  and  $\gamma'=1$ . (b) Heating section (HS), cooling section (CS) and denuder section (DS) output thermograms for  $20 \mu\text{g}/\text{m}^3$  aerosol mass loading. Baseline case:  $C^*=10 \mu\text{g}/\text{m}^3$ ,  $d_{p0}=100 \text{ nm}$ ,  $D_i=5 \times 10^{-6} \text{ cm}^2/\text{s}$  and  $\gamma'=1$ . (data provided represent the upper estimate for re-condensation)

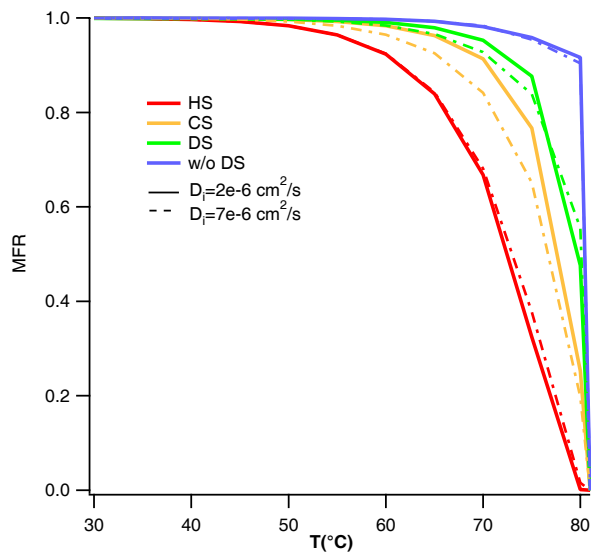


**Figure S5.** Output thermograms and recondensation fraction for the heating section (HS), cooling section (CS), denuder section (DS) and equivalent configuration without denuder section (w/o DS) for different diffusion coefficients. Baseline case:  $C_{OA} = 400 \text{ } \mu\text{g}/\text{m}^3$ ;  $C^* = 0.01 \text{ } \mu\text{g}/\text{m}^3$ ,  $d_{p0} = 100 \text{ nm}$ ,  $D_i = 5 \times 10^{-6} \text{ cm}^2/\text{s}$  and  $\gamma = 1$ . (data provided represent the upper estimate for re-condensation)

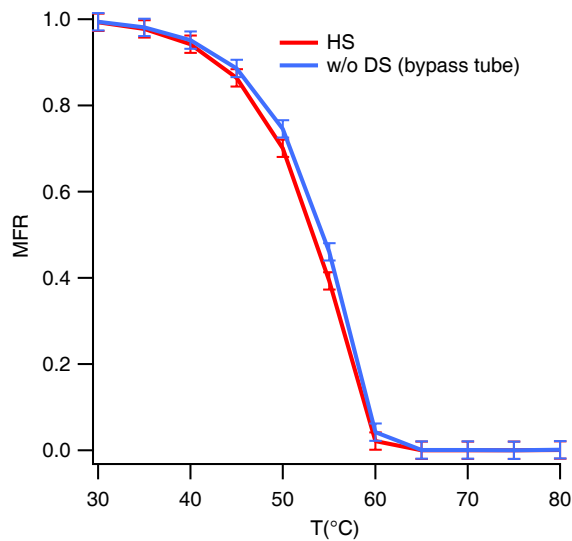


**Figure S6.** Modeled thermograms of adipic acid aerosol in the re-condensation test experiments by Saleh et al. (2011) (initial aerosol loading:  $287 \text{ } \mu\text{g}/\text{m}^3$ , flow=1 lpm, by-pass tube length=2 m). HS: heating section output thermogram. w/o DS: output thermogram of cooling section without denuder. Error bars indicate the uncertainty in measurements by Saleh et al. (2011). Re-condensation is negligible in this particular case due to the short residence time of the fluid in the by-pass tube without denuder (3.74 s) and the low accommodation coefficient of the aerosol sample ( $\gamma = 0.1$ ). (data provided correspond to upper estimate for re-condensation)

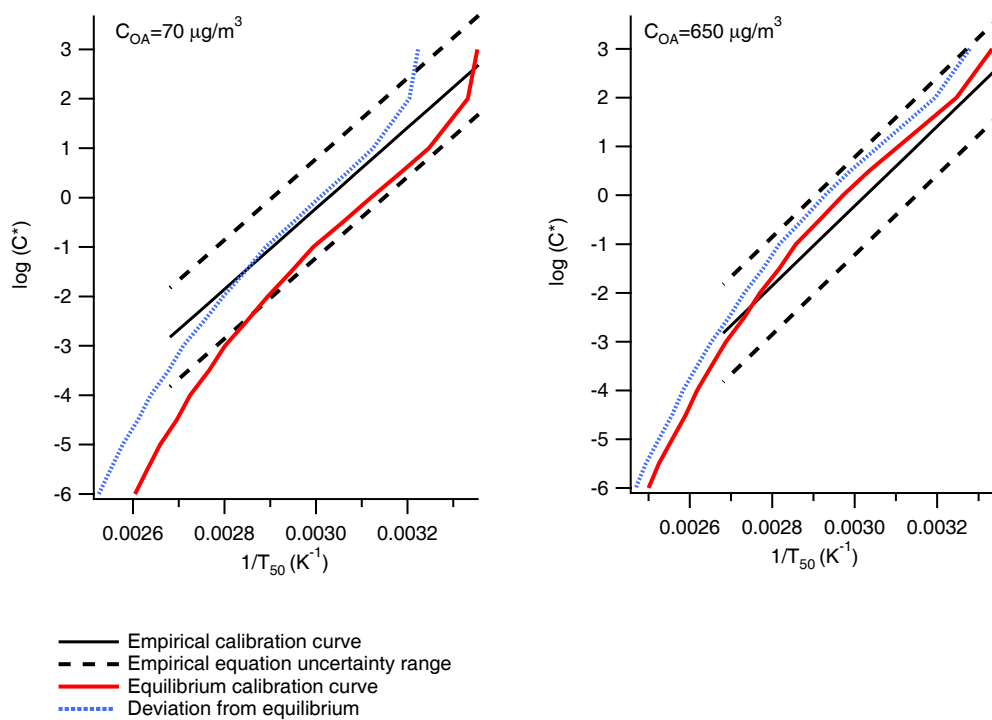


**Fig S7.** Deviation of calibration curve from the equilibrium and empirical curves in experiments with lubricating oil aerosol at 70 and 650  $\mu\text{g}/\text{m}^3$  mass loading.

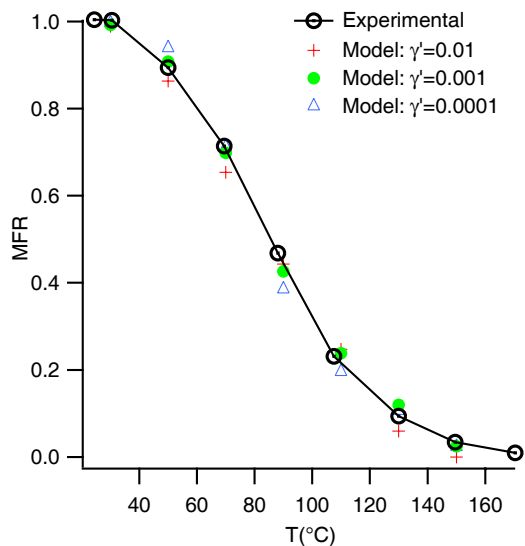


**Fig S8.** Kinetic model fitting to experimental thermogram of  $\alpha$ -pinene SOA at 500  $\mu\text{g}/\text{m}^3$  initial aerosol loading (Cappa and Wilson, 2011). A good agreement between the model and experimental data is achievable for different accommodation coefficient values.